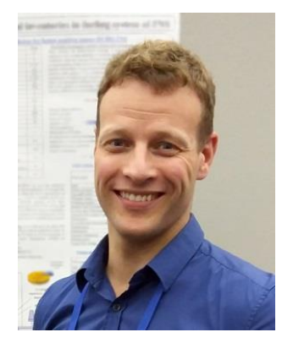

S.S. Ananyev, E. D. Dlougach, A.V. Klishchenko
National Research Center Kurchatov Institute, Moscow, Russia
Ananyev_SS@nrcki.ru

NIBS 2020 online

The 7th International symposium on Negative Ions, Beams and Sources (NIBS'20)
1-11 September 2020

KURCHATOV INSTITUTE
NATIONAL RESEARCH CENTRE

Analysis of the DEMO-FNS magnetic field influence on the neutral beam injection and methods of injectors shielding

Introduction

Steady-state operation mode of a fusion neutron source (FNS) will require plasma heating and maintaining the current in it by fast atoms beam injecting. The DEMO-FNS project assumes the use of six injectors providing additional heating power up to 30 MW at an atomic energy of 500 keV. As a prototype for the DEMO-FNS injector, an injector developed in detail for the ITER project can be used, with the injector layout retained, but changes in individual components, which is caused by the difference in beam energy and power. Inside these components, there are very strict restrictions on the magnetic field magnitude (the flux density should be below a certain value along the path of ion movement and even lower in the neutralization region). To achieve these characteristics in an environment with a high scattered field due to the magnetic system of the facility, which includes the coils of the poloidal and toroidal fields, the central solenoid and the plasma itself, additional shielding of the injectors is provided. At this stage, we expect that the proposed design will allow obtaining the required magnetic field values only by passive injectors shielding due to a case made of a ferromagnetic material with a high magnetic permeability index.

DEMO-FNS neutral beam injection system

The system of six injectors will provide the steady-state plasma heating and current drive in the DEMO-FNS plasma, thereby creating conditions for the continuous operation of the entire facility. Since the operation of each individual injector should be periodically terminated for a short time to regenerate gas from cryopanels, the continuous injection is provided by the simultaneous operation of four injectors, while the fifth one, by turns, operates in the cryopanel regeneration mode. The sixth injector is provided for being in the operational reserve, routine servicing or under repair. Obviously, each injector should provide the maximum duration of injection.

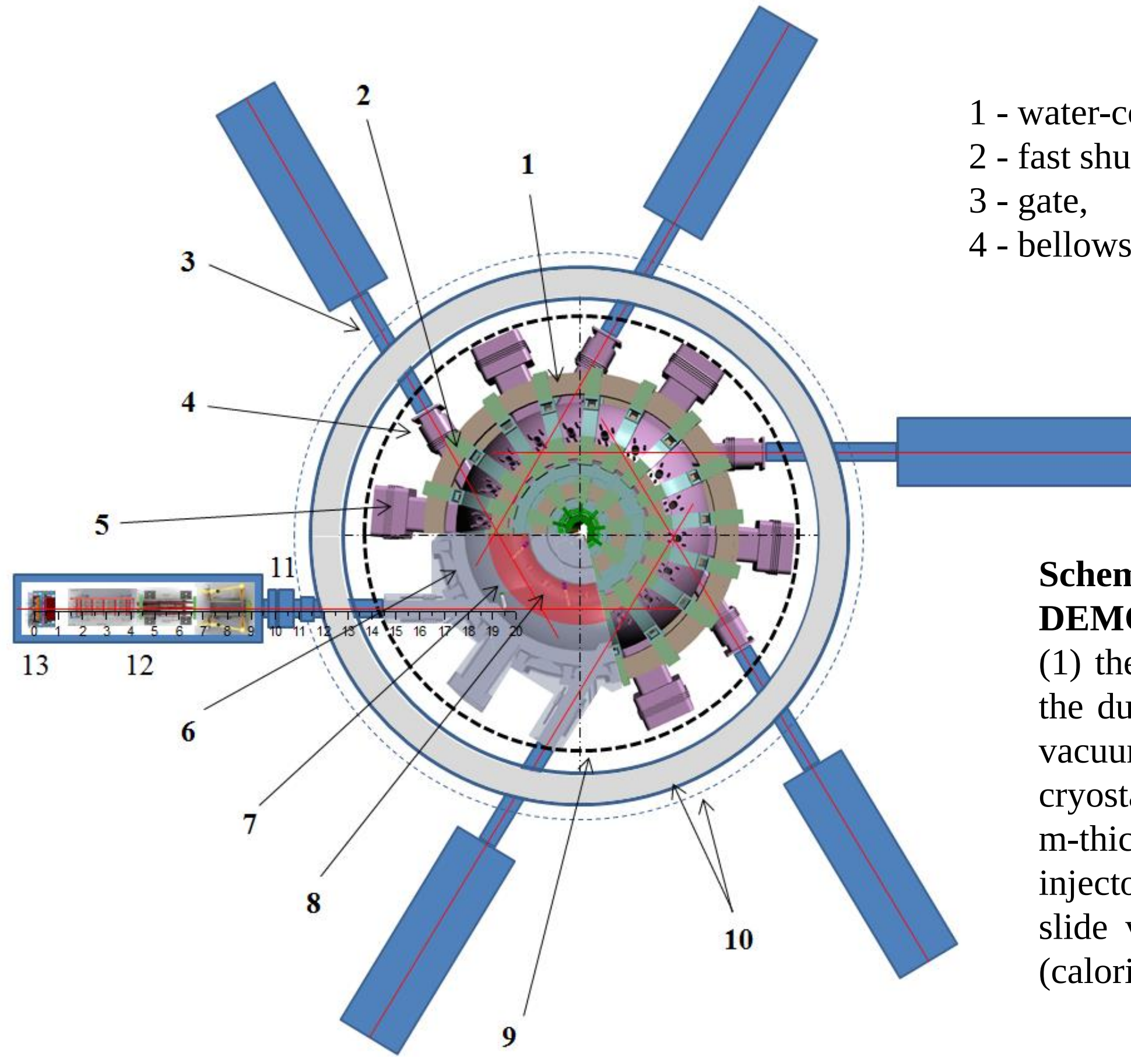

1 - water-cooled diaphragm "scraper",
2 - fast shutter,
3 - gate,
4 - bellows

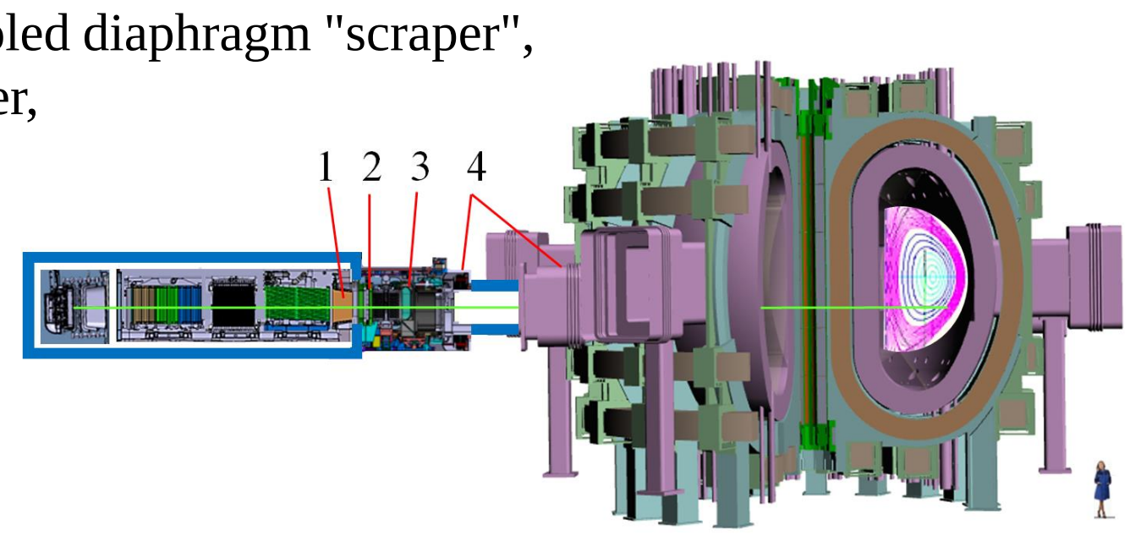

Schematic of the injector arrangement relative to the DEMO-FNS vacuum chamber: (1) the poloidal field coils; (2) the toroidal field coils; (3) the duct; (4) the NBI port; (5) the equatorial port; (6) the vacuum chamber; (7) the first wall; (8) plasma; (9) the cryostat; (10) solid and dotted lines correspond to the 1.25-m-thich and 2.0-m-thick shields, respectively; the beam injector consists of the following components: (11) the slide valve, shutter and bellows; (12) the beam receiver (calorimeter), RID and neutralizer; and (13) the ion source.

Requirements for the magnetic field components attenuation system

The requirements for the DEMO-FNS NBI magnetic field components attenuation system were obtained in the injection path optimization calculations process, performed earlier. The most stringent condition for the admissible field value $Bz < 10^{-4}$ T relates to the region from the ion accelerator exit to the neutralizer and in it. In the area between the neutralizer output and the RID entrance, the requirements for the field value are lower - it should be $< 3\cdot10^{-3}$ T. The field strength in the atomic receiver and scraper (the diaphragm element at the injector out) region is an order of magnitude lower than in the neutralizer. Requirements for the magnetic field magnitude in the duct are not established, since the magnetic field presence in this area has a positive effect on the loads distribution along the duct walls.

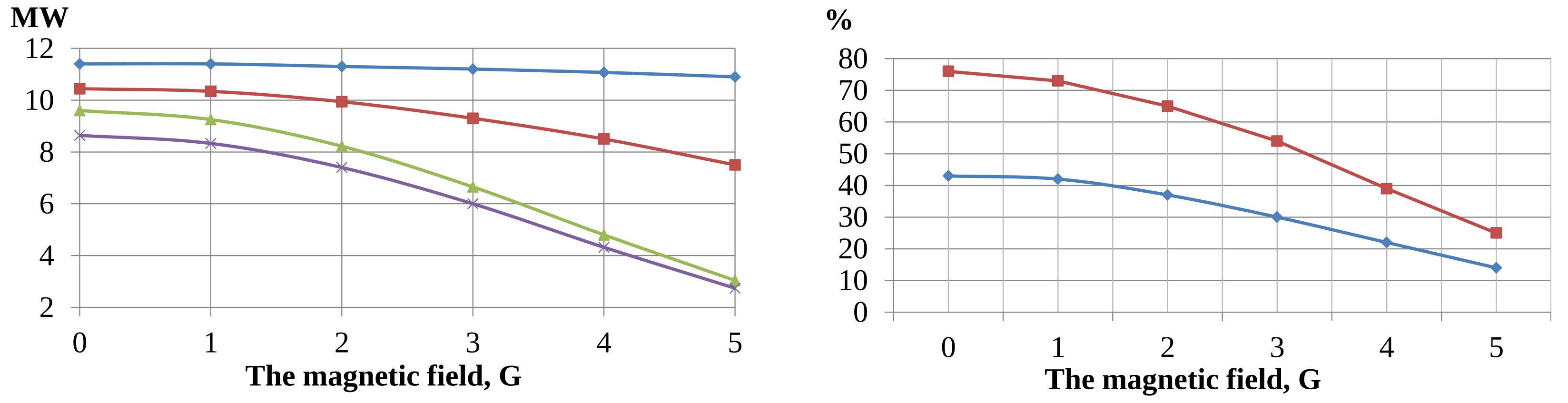

(left) Changes in the neutral beam power along the injection track and (right) efficiencies of the beam ◆ transformation (P_{inj}/P_0) and 🟥 transport (P_{inj}/P_N) in different operating modes (with allowance for the beam losses due to the reionization) at different vertical magnetic fields (along the beam path segment from the ion source to the RID). The beam focusing is assumed to be perfect. Two-channel scheme is considered. Different colors correspond to the following beam powers: 🟦 power at the neutralizer exit, 🟥 power at the RID exit, 🟩 power at the duct exit, and 🟪 power with allowance for the 10%-losses due to reionization

DEMO-FNS facility model for the magnetic field calculating

NBI injector case is located at a considerable distance from the magnetic system (the length of the beam line is > 20 m) - in this area the magnetic field generated by the poloidal coils has the greatest influence, however, we consider it important to take into account all sources for correct calculation: poloidal coils, toroidal coils, central solenoid and plasma.

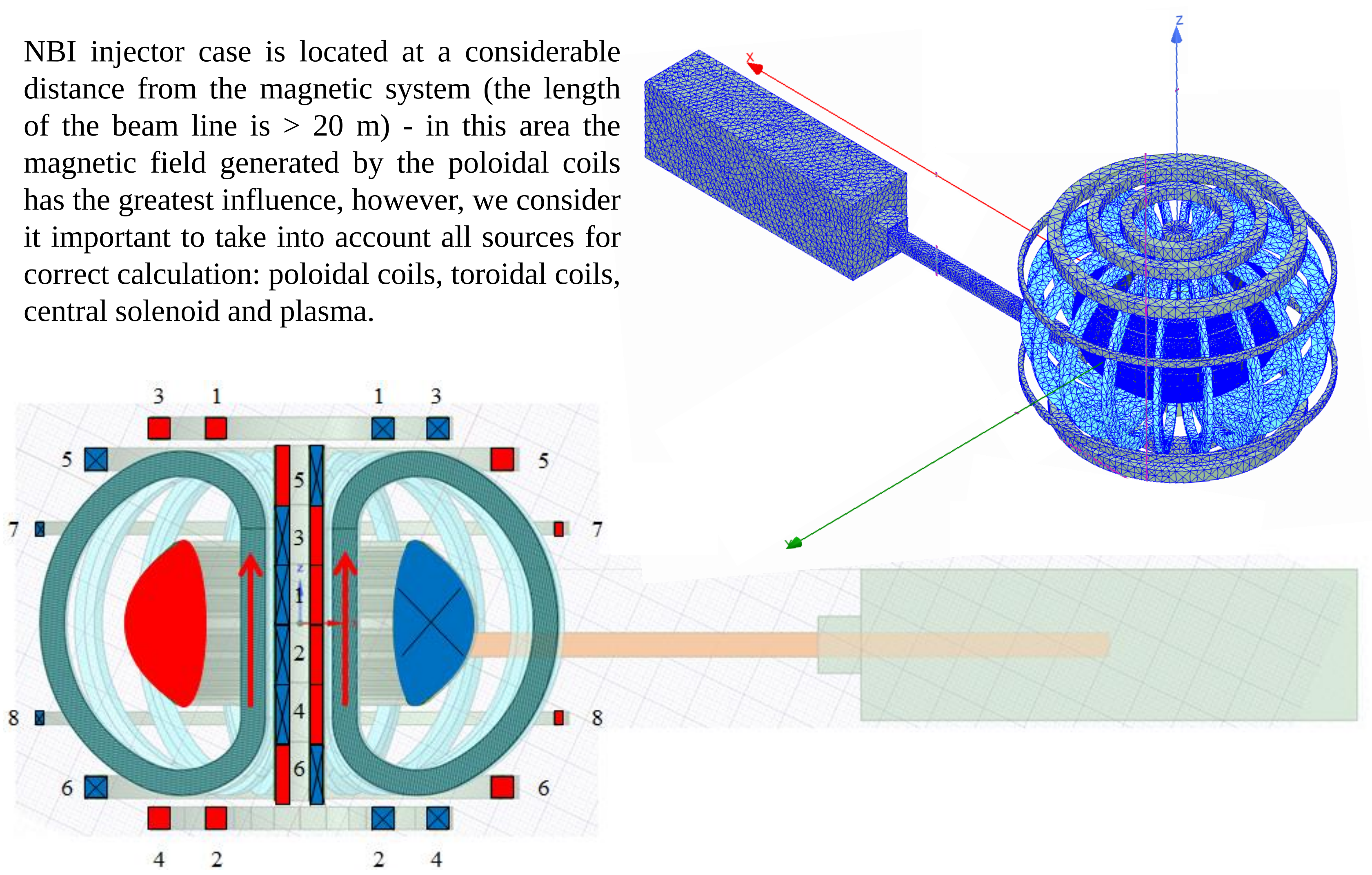

Coils	Current (kA)
Toroidal coil №1-18	4300
Poloidal coil №1	8026
Poloidal coil №2	8026
Poloidal coil №3	6105
Poloidal coil №4	6105
Poloidal coil №5	5881
Poloidal coil №6	5881
Poloidal coil №7	1360
Poloidal coil №8	1360
Plasma	5000
Solenoid – section № 1	11509
Solenoid – section № 2	11509
Solenoid – section № 3	2148
Solenoid – section № 4	2148
Solenoid – section № 5	965.7
Solenoid – section № 6	965.7

We calculated the dependences of three components *Bx*, *By*, *Bz* - the projections of the magnetic induction vector on the plane perpendicular to the beam direction, on the distance X - without shielding.

The magnetic induction vertical component *Bz* in the injector region is maximum.

Passive magnetic shielding system optimization

A injector magnetic shield model was created - a multilayer box with external dimensions of **11.5 m × 3.5 m × 3 m** from a material with high relative magnetic permeability and variable layers thickness, vacuum gaps between them and their number. Thus, a passive shield is a set of nested boxes with the same wall thickness with certain vacuum gaps between successively nested boxes, by analogy with a **"matryoshka"**.

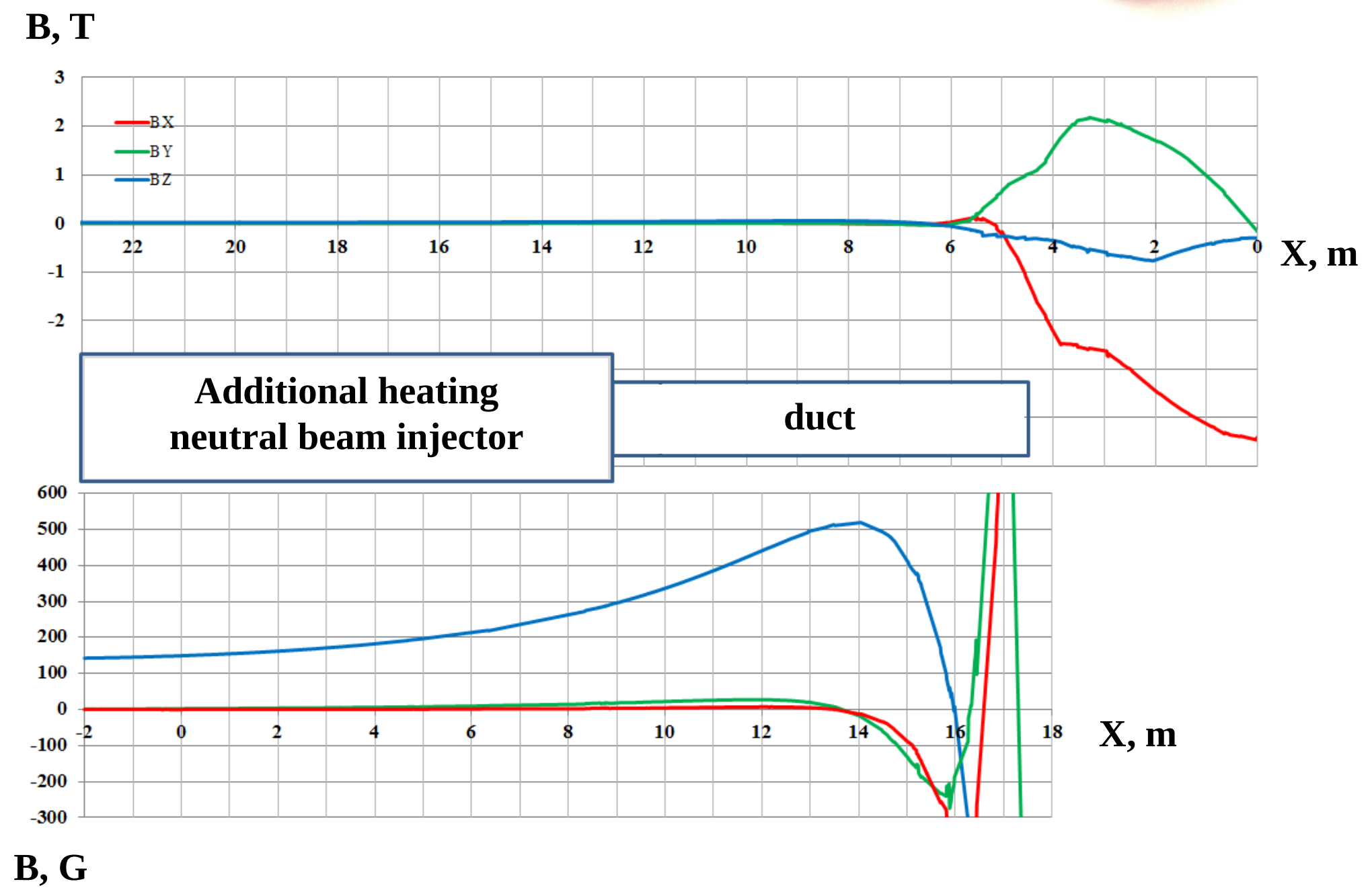

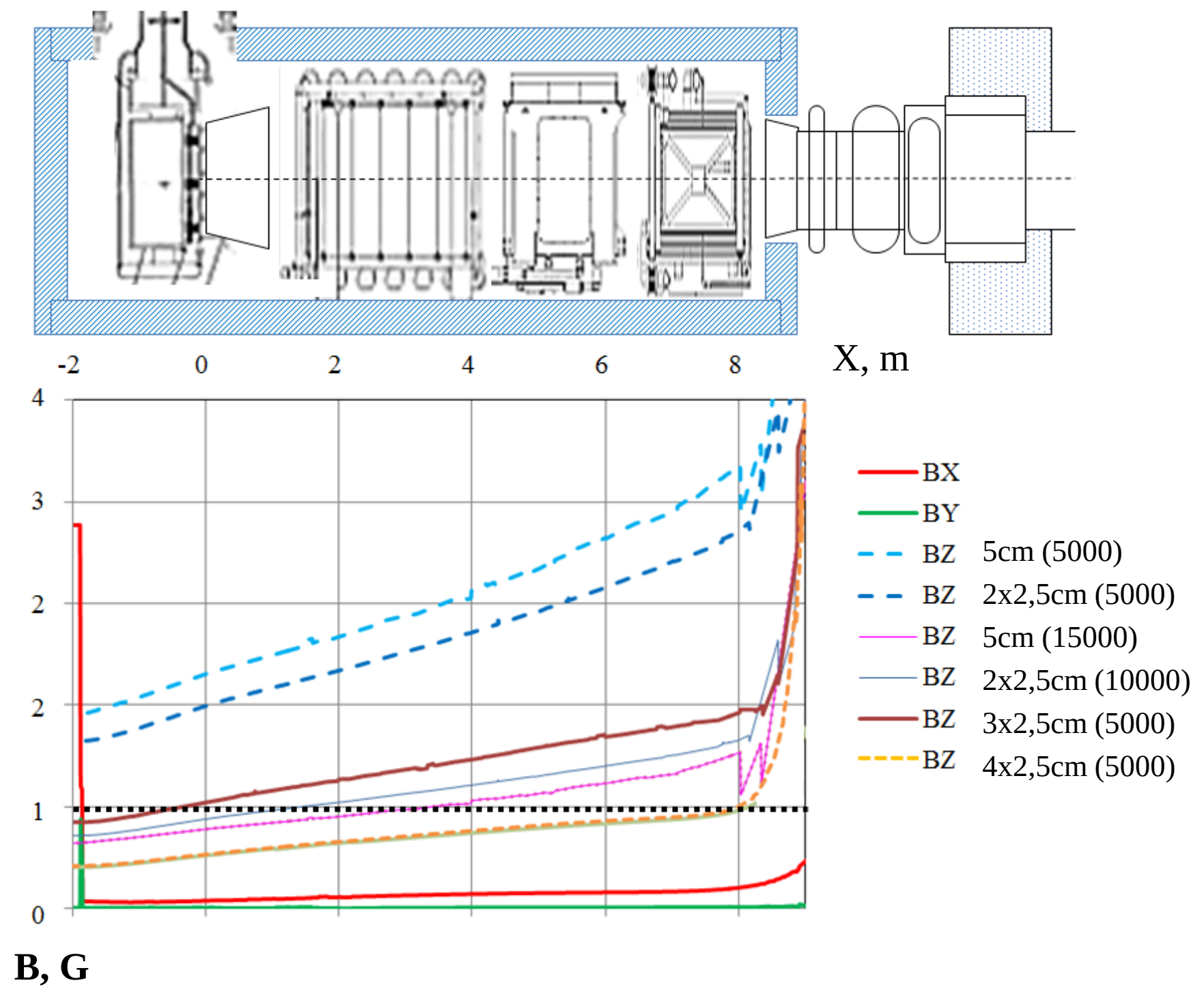

Variants of one-layer shielding with a thickness of 5 cm, as well as two-, three- and four-layer ones with different layer thicknesses and various vacuum gaps between them were considered.

A calculations serie was performed to select the optimal layer thicknesses and vacuum gaps between layers for optimal passive suppression of the magnetic induction vector projection on planes perpendicular to the beam direction. As already noted, the main criterion is the field value in the region from the ion source and in the neutralizer, which should not exceed 1 G.

The most suitable options turned out to be a single-layer with a 5 cm thickness and a relative magnetic permeability equal to 15000, two-layer with a layer 2.5 cm thickness and a relative magnetic permeability equal to 10,000, and a four-layer with 2.5 cm layers and a relative magnetic permeability equal to 5000. In this case, the requirements for the magnitude in the most critical injector regions - the neutralizer and the ion source are satisfied only by the last option and partially by the first.

Particle trajectories calculation in obtained magnetic fields conditions with reionization

The ion trajectories and the corresponding thermal loads distribution are determined by the magnetic field configuration in the beam reionization region. The most "dangerous" is the vertical magnetic field component Bz, which causes a horizontal ions deflection leaving the source until they are neutralized, i.e. in the section from the source to the neutralizer outlet, and can also lead to incomplete residual ions interception in the ion dump. The magnetic field also distorts the internal angular beamlets distribution.

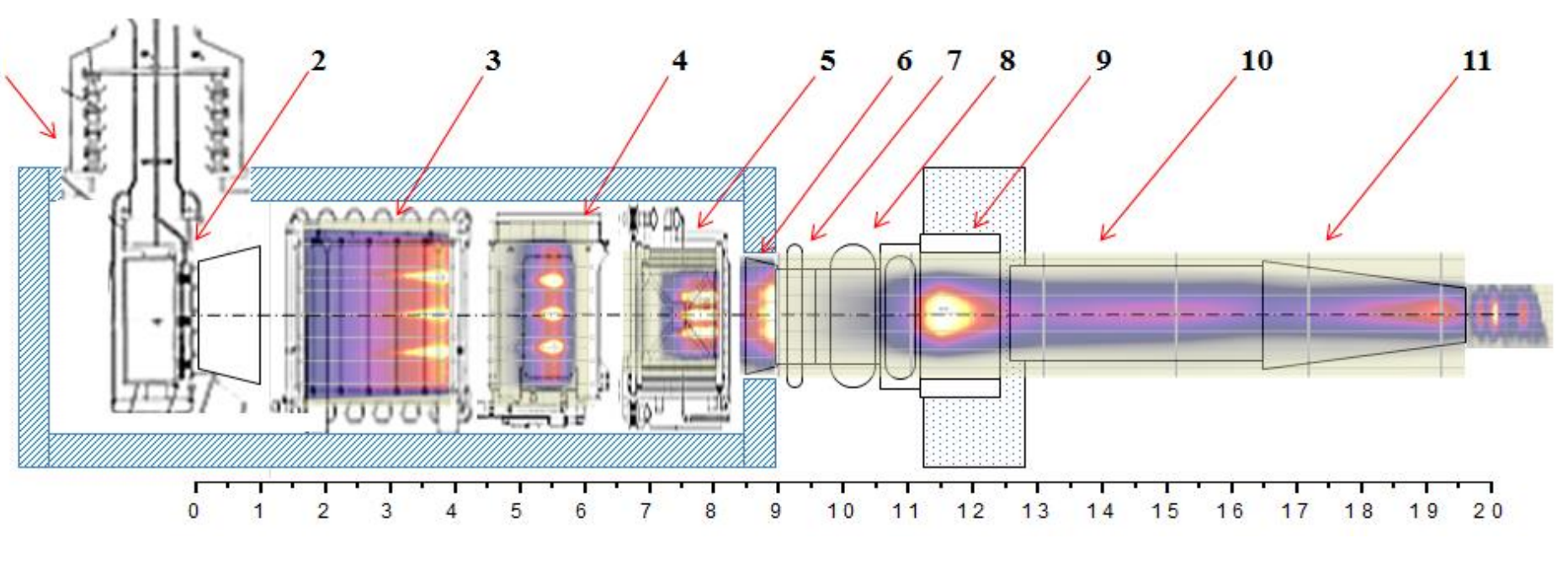

(1) high-voltage bushing of the ion source, (2) the negative ion accelerator, (3) the neutralizer, (4) the residual ions dump, (5) the atom receiver (calorimeter), (6) the scraper, (7) the fast shutter, (8) the slide valve, (9) the bellows unit, (10) the duct, and (11) the duct liner.

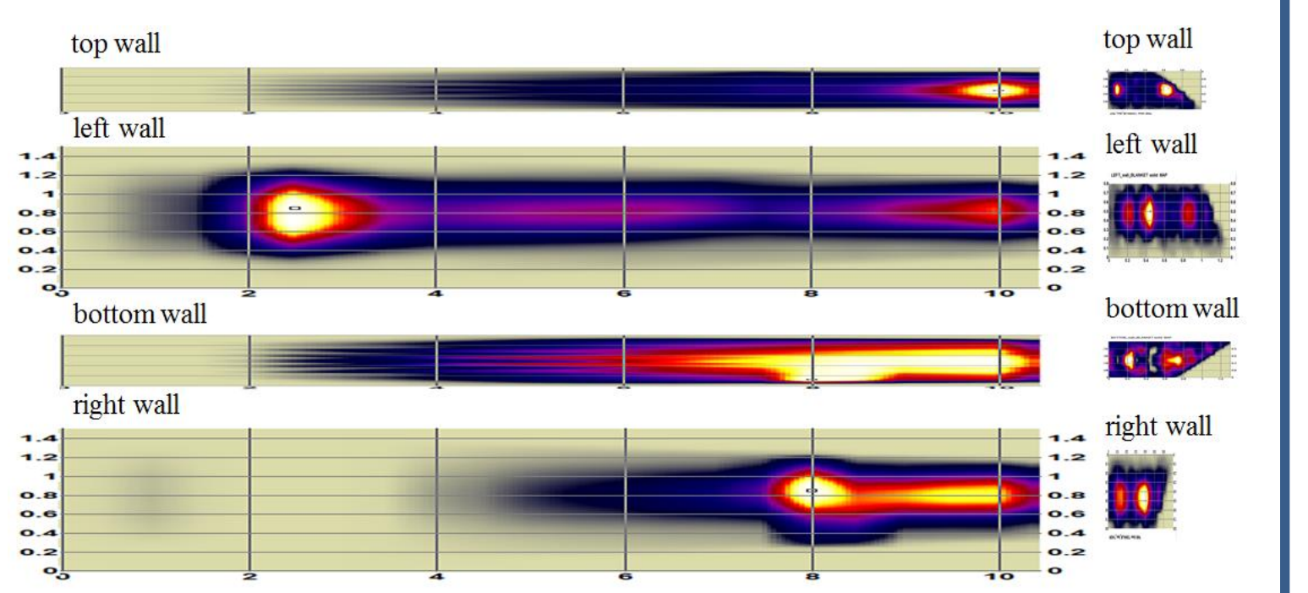

Duct side panels layout. There are no heat removal panels inside the vacuum chamber - in the hybrid blanket area their role is played by blanket elements.

Changes in the beam power along the injection track and the distribution of the loads and peak power densities between its components. The beam power at the ion source exit is 20 MW, and the neutralization efficiency is 0.6. The beam divergence is 7 mrad and the halo radiation divergence is 30 mrad. The last column takes into account the magnetic field (MF) influence - the horizontal deflection is -2mrad, so that the effects of deflection and magnetic field (MF) add up and not compensate (worst case).

The angle of horizontal/vertical deflection of the beam axis, mrad	0/0	2/4	-2/4 (+MF)
Beam load power in the neutralizer, MW	1.18	1.25	1.24
Peak power density at the end elements of the neutralizer, MW/m^2	1.4	1.9	1.75
Peak power density on the neutralizer channel wall, MW/m^2	0.16	0.21	0.26
Neutral beam power at the neutralizer exit, MW	11.29	11.25	11.13
Neutral beam power loss inside the RID, MW	0.63	0.69	0.77
Total power released in the RID (atoms + ions), MW	8.16	8.19	8.6
Peak power density on the exposed edge of the RID panel, MW/m^2	2.6	3.30	4.8
Peak power density on the RID panel, MW/m^2	3.7	4.0	4.4
Neutral beam power at the RID exit, MW	10.67	10.56	10.0
Peak power density on the calorimeter panel, MW/m^2	11.25	11.25	11.0
The beam power intercepted by the scraper, MW	0.105	0.12	0.22
Peak power density on the scraper wall, MW/m^2	0.14	0.26	0.53
Beam load power on the walls of the duct liner, MW	0.83	1.0	1.64
Peak power density on the side wall of the liner, MW/m^2	0.21	0.37	0.73
Peak power density on the upper wall of the liner, MW/m^2	0.1	0.38	0.54
Neutral beam power introduced into the plasma, MW:			
- excluding losses due to reionization	9.73	9.43	9
- with allowance for the 10%-losses due to reionization	8.76	8.49	8.02

Conclusion

An electromagnetic analysis of the effectiveness of such a screen was performed using 3D modeling using the ANSYS code. For this, a computational finite-element model DEMO-FNS was created, which includes a vacuum volume in which an electromagnetic system is located and one of 6 heating injectors. The magnetic field components values on the injection axis were calculated without shielding the injector region. It was shown that the vertical field component *Bz* in the injector region is maximum and is in the range of *300-150 G*.

Variants of single-layer shielding using various materials, and multilayer ones: two-, three- and four-layer with different layer thicknesses and vacuum gaps between them were considered. By choosing the optimal thicknesses of layers and gaps, the projection of the magnetic induction vector on the plane perpendicular to the beam direction was suppressed to acceptable values in the region of the injector components. It was shown that by increasing the shield layers number made of a material with a lower relative magnetic permeability value, one can achieve better shielding than when using one material layer with a larger relative magnetic permeability value of the same total thickness.

The BTR code was used to calculate the motion of particles in the conditions of the obtained magnetic fields, taking into account reionization along the entire injection path length. The distributions of loads and power losses on the injector components and the transverse beam power dynamics are obtained. Loads calculations have shown that for a given magnetic field distribution, the loads on the duct are significantly uneven, which together with the reionized particles fluxes focusing in magnetic fields, is the greatest danger for heat removal. These results will be used later in the injector case and the duct engineering design.

The work was supported by the NRC "Kurchatov Institute (14.08.2019 № 1805).

Publications on the fusion neutron source DEMO-FNS NBI system

S.S. Ananyev, A. A. Panasenkov, A. I. Krylov, E. D. Dlougach, and B. V. Kuteev «Concept of Plasma Heating and Current Drive Neutral Beam System for Fusion Neutron Source DEMO-FNS» // Physics of Atomic Nuclei, 2019, Vol. 82, No. 7, pp. 981–990. DOI: 10.1134/S1063778819070020

NIBS'18 poster presentations